

Anti-Resonance and the "0.7 Anomaly" in Conductance through a Quantum Point Contact

Ye Xiong,¹ X. C. Xie,^{1,2} and Shi-Jie Xiong³

¹Department of Physics, Oklahoma State University, Stillwater, Oklahoma 74078

²International Center for Quantum Structures and Institute of Physics,
The Chinese Academy of Sciences, Beijing 100080, P.R. China

³Department of Physics, Nanjing University, Nanjing 210093, China

(dated: April 14, 2024)

We investigate the transmission of electrons through a quantum point contact by using a quasi-one-dimensional model with a local bound state below the band bottom. While the complete transmission in lower channels gives rise to plateaus of conductance at multiples of $2e^2/h$, the electrons in the lowest channel are scattered by the local bound state when it is singly occupied. This scattering produces a wide zero-transmittance (anti-resonance) for a singlet formed by tunneling and local electrons, and has no effect on triplets, leading to an exact $0.75(2e^2/h)$ shoulder prior to the first $2e^2/h$ plateau. Formation of a Kondo singlet from electrons in the Fermi sea screens the local moment and reduces the effects of anti-resonance, complementing the shoulder from 0.75 to 1 at low temperatures.

PACS numbers: 73.23.Ad, 72.10.Fk, 72.15.Gd

The quantization of conductance in mesoscopic systems has been observed in quantum point contacts (QPC) where a series of plateaus at multiples of $2e^2/h$ appears in curves of conductance G versus gate voltage V_g [1, 2]. Prior to the first integer plateau, a shoulder of $0.7(2e^2/h)$ has often been observed and is called the "0.7 anomaly" [3, 4, 5, 6]. Considerable experimental and theoretical efforts have been devoted to understanding this anomaly [7, 8, 9, 10, 11]. In Ref. 10 it is suggested that the anomaly originates from the 3:1 triplet-singlet statistical weight ratio if two electrons form bound states by some attractive interaction and the triplet has a lower energy. From calculations for two electrons in the Hubbard model or the Anderson Hamiltonian, two resonance peaks in transmission spectrum are shown, corresponding to singlet and triplet states with weights 0.25 and 0.75 [11]. Some attention has been focused on the Kondo effect in such systems [12, 13]. In a recent experiment the temperature and magnetic-field dependence of the differential conductance was investigated in detail to highlight the connection to the Kondo problem [14], and subsequently a theoretical study was carried out in further support of Kondo physics in QPC [15].

Since relevant states undergo empty, single and double occupations even within the width of one plateau or shoulder, including global charge variations and fluctuations in calculations is important. The "0.7 anomaly" appears only prior to the first integer plateau, and only at relatively higher temperatures, for which the intensity of the Kondo effect is negligible. The shape of the shoulder is much different from the two resonance peaks of the singlet and triplet states [11], and there is no evidence of the attractive interaction from which two-electron bound states can be formed [10]. To address the above mentioned questions, in this Letter we theoretically study the

transport through a quantum point contact (QPC) by using a model which includes the Coulomb interaction, the charge fluctuations, and the multi-channel structure on an equal footing. By using the singlet-triplet representation to label spin states of the tunneling electron and the local electron, we show a wide anti-resonance for the singlet channel near the band bottom, giving rise to the 0.75 shoulder. The shoulder is complemented to 1 by the formation of a Kondo singlet at low temperatures, and manifests itself at higher temperatures when the Kondo singlet collapses. Thus, the role of the Kondo singlet is to suppress the anti-resonance, quite different from the Kondo physics discussed in Ref. [15]. A simple scaling curve for conductance is obtained and is found to compare well with the experimental one. The results provide consistent explanations for a wide range of characteristics observed in experiments.

A QPC can be described with a narrow and short bar connected to the left and right leads which serve as reservoirs. Thus, one obtains several continuous 1D subbands. Some local levels, may be virtual bound states [15], can be created by the specific QPC geometry. These states are isolated from the leads and should not be included in the band continuum. The potential of the bar area, including both the band continuum and the local levels, is tuned by the gate voltage. The single-electron energies of subbands and levels are shown in Fig. 1(a). We include on-level Coulomb repulsion U of electrons confined in one local state. In equilibrium the Fermi energy of reservoirs is fixed and we set it as the energy zero. The occupations of levels is controlled by tuning the gate voltage. In Figs. 1(b), 1(c) and 1(d) we show the empty, single and double occupations of the level nearest the band bottom. When the Fermi level crosses the band bottom, the first subband contributes to the conductance and the first

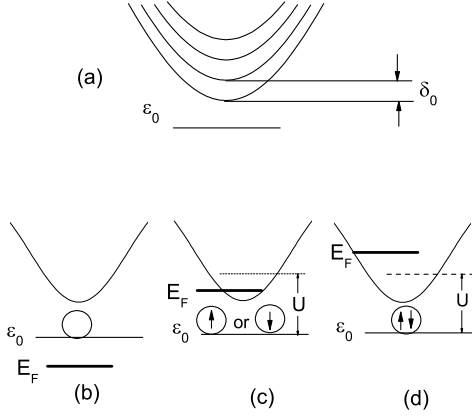


FIG. 1: (a) Sketchy illustration of dispersion relation of 1D subbands and local levels. ϵ_0 is energy spacing between subbands, and δ_0 is the position of the local level. (b) Empty level. E_F denotes the Fermi level. (c) Singly occupied level. (d) Doubly occupied level.

plateau appears. At this moment most of the local levels are fully occupied and have no effect on the transport, except the one closest to the band bottom which may be singly occupied due to the on-level interaction. It is sufficient to include this level in our model. By tuning V_g further this level is also fully occupied and the plateau structure is determined only by the subbands.

The Hamiltonian of the system can be written as

$$\begin{aligned}
 H = & \sum_{m, i; j} t_0 (a_{m, i; j}^\dagger a_{m, i+1, j} + \text{H.c.}) \\
 & + \sum_{m, i; j} [(m-1)\epsilon_0 - eV_g] a_{m, i; j}^\dagger a_{m, i; j} \\
 & + \sum_{i=0} t^0 (a_{1,0}^\dagger d + \text{H.c.}) + \sum_{i=0} (\epsilon_0 - eV_g) d^\dagger d \\
 & + U d_n^\dagger d_n d_\#^\dagger d_\#; \quad (1)
 \end{aligned}$$

where $a_{m, i; j}$ and d are the annihilation operators of electrons on the i th site of the m th continuum channel and at the local state, respectively, with j being the spin index. ϵ_0 is the energy spacing between subband bottom s . ϵ_0 stands for the position of the local level. t_0 is the hopping integral of the channels, and t^0 is the coupling of the lowest channel and the bound state at a site ($i=0$). Only the coupling of the local level to the lowest channel ($m=1$) is considered, because local level coupling has no effect on the transmission in higher channels due to the double occupation.

For $V_g = 0$ and at the zero temperature, the potential is too high and the states in the bar, including the local

state and the continuum chains, are empty. With increasing V_g , the local state becomes singly occupied in the range of $0 < eV_g < \epsilon_0 + U$. For $eV_g > \epsilon_0 + U$, it is doubly occupied and has no effect on the conductance. On the other hand, the m th continuum channel gives $2e^2/h$ contribution to the conductance if $eV_g > (m-1)\epsilon_0 - 2t_0$, because in this case the Fermi level is higher than the bottom of this subband. This provides the integer plateaus in the $G-V_g$ curves with plateau width $\epsilon_0 = e$.

Since the local level is below the bottom of the whole band continuum, the tunneling in the first channel is affected by its charge and spin states. There are 4 states of the local level: the empty, $|j_1 i = j_0 i\rangle$, the spin up and down single occupation, $|j_2 i = j^{\uparrow} i\rangle$ and $|j_3 i = j^{\downarrow} i\rangle$, and the double occupation, $|j_4 i = j^{\uparrow\downarrow} i\rangle$. If an electron is injected into the channel, it will be scattered by the state on the local level. At first we consider only the tunneling and local electrons and ignore the other electrons in the Fermi sea. These considered electrons form a many-body state

$$|j i\rangle = \sum_{n=1}^N \sum_{i; j} X_{n;1;i;j}^j |j_1 i = j_0 i\rangle + \sum_{n=1}^N \sum_{i; j} X_{n;1;i;j}^{\uparrow} |j_2 i = j^{\uparrow} i\rangle + \sum_{n=1}^N \sum_{i; j} X_{n;1;i;j}^{\downarrow} |j_3 i = j^{\downarrow} i\rangle + \sum_{n=1}^N \sum_{i; j} X_{n;1;i;j}^{\uparrow\downarrow} |j_4 i = j^{\uparrow\downarrow} i\rangle \quad (2)$$

where $|j i; i\rangle$ is the orbital at site i with spin j in the first channel, and $p_{n;1;i;j}$ is the corresponding coefficient. By applying the Hamiltonian on $|j i\rangle$ one obtains the Schrodinger equations for the coefficients. These equations can be expressed with an equivalent single-particle network in which every site represents a combination of indices $(n;1;i;j)$ of the coefficients [16]. In the present case the network is an 8-channel one where every channel stands for a combination of n and j , and a site in a channel corresponds to a coordinate i in the chain. In the network the channels with $(n=2; j=\uparrow)$ and $(n=3; j=\downarrow)$, and the channels with $n=1;4$, corresponding to the empty and doubly occupied local states, are independent. The other 2 channels are connected at site $i=0$ but can be easily decoupled with the transformation $\tilde{j}_2 i = \frac{1}{\sqrt{2}}(j_2 i - j_1 i; \# i - j_3 i - j_1 i; \# i)$ and $\tilde{j}_3 i = \frac{1}{\sqrt{2}}(j_2 i - j_1 i; \# i + j_3 i - j_1 i; \# i)$. The final network with 8 independent channels is shown in Fig. 2. For single occupation there is one singlet channel with one scatterer (6) and three pure triplet channels (3, 4, and 5) without scattering by the local level. Different from Ref. [10], the singlet-triplet notation used here is merely to label spin states of the tunneling and local electrons that are not bound together. For $m > 1$ and for the non-scattering pure channels of $m=1$, the transmission coefficient is

$$T_m(\epsilon) = \begin{cases} 1; & \text{for } j = (m-1)\epsilon_0 + eV_g < 2t_0; \\ 0 & \text{otherwise.} \end{cases} \quad (3)$$

where ϵ is energy of the injected electron. For the singlet

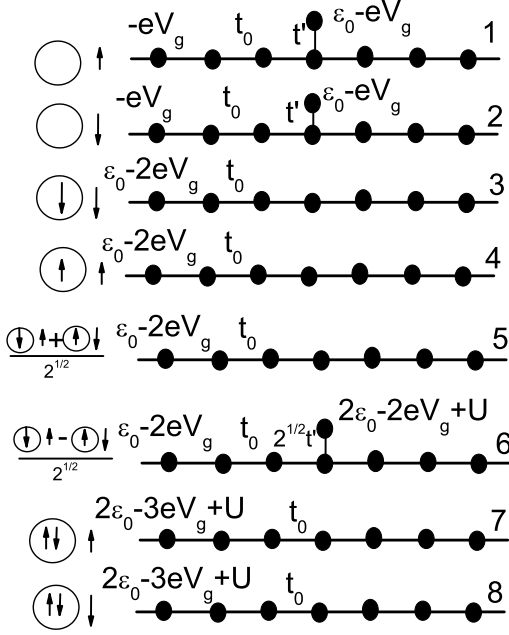


FIG. 2: Eight independent channels for a tunneling electron. The state of the local level is illustrated by circles, and the spin of the tunneling electron is represented by an arrow outside the circle.

(empty) channel of $m = 1$,

$$s(e) = \frac{4 [u_s(e)]^2 \cos(k)^2 \sin^2(k)}{v_s^4(e) + 4 [u_s(e)]^2 \cos(k)^2 \sin^2(k)} \quad (4)$$

for $j + eV_g j < 2t_0$ and $s(e) = 0$ otherwise, where k is the momentum of the tunneling electron determined by $\hbar k \cos(k) = eV_g$, and $u_s = (t_0 + U)t_0$, $u_e = t_0$, $v_s = 2t_0$, $v_e = t_0$.

For the singlet channel the scatterer produces an anti-resonance at $\epsilon_0 - eV_g + U$ with a zero transmission coefficient at the minimum and with semi-width $t_0^2 = t_0 j \sin(k) j$. Near the subband bottom where we focus, $\sin(k) \approx 0$, so the width of the dip is extremely large even though t_0 may be much smaller than t_0 . As a result, the dip of s develops to a flat plateau with nearly zero height. This is different from the results of Ref. [11] where the singlet and triplet states give two separate resonance peaks with different weights. Without the magnetic field and ignoring the effects of other electrons, in the range of single occupation commensurate the conductance is governed by $e^2/2h$ times the sum of the transmission coefficients of the singlet and triplet channels which are non-zero only for the tunneling electron with energy higher than the subband bottom. Here the prefactor $1/2$ stands for the weight of one spin state of the local electron. As mentioned above, $\epsilon_0 < 2t_0$, so

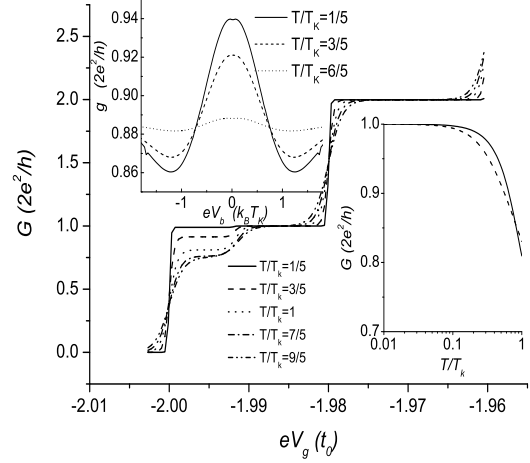


FIG. 3: Linear conductance as a function of the gate voltage. The parameters are: $\epsilon_0 = 0.02t_0$, $U = 0.016t_0$, $\epsilon_0 = 2.008t_0$, $T_K = 0.0005t_0$ and $t_0^0 = 0.05t_0$. Upper inset: Differential conductance as a function of bias voltage for $eV_g = 1.993t_0$. Lower inset: Linear conductance as a function of scaled temperature T/T_K . Solid line: The calculated conductance. Dashed line: The experimentally fitted conductance.

$\epsilon_0 + U$ may be above the subband bottom. Thus, in the range of $2t_0 < eV_g < \epsilon_0 + U$ conductance plateaus at height $0.75(2e^2/h)$. For $eV_g > \epsilon_0 + U$, the conductance is dominated by the double-occupation channels (7 and 8 in Fig. 2), leading to a jump from 0.75 to 1 at $eV_g = \epsilon_0 + U$. This is the origin of the 0.7 anomaly within our model.

Now we consider the effect of the electrons in the Fermi sea. It is known that at low temperatures the electrons from Fermi sea are coupled with the local electron to form a Kondo singlet. In this case the local state is screened by the Fermi electrons and is no longer available for the injected electron in the singlet channel, resulting in the disappearance of the side-coupled scatterer for this channel. This removes the anti-resonance and enhances the transmission coefficient from nearly zero to one. If the probability of annihilating the Kondo singlet is p_k , the average transmission coefficient of the singlet channel is $s_s = (1 - p_k) + p_k s_s$. We choose $p_k = \tanh(T/T_K)^2$. This simple form reflects the physics that at low temperature the Kondo singlet peak in the spectral density goes as $1/T^2$ [18]. The formation of the Kondo singlet has no effect for the triplet channels since they are without scattering.

Combining all the contributions, the linear conductance at temperature T can be calculated as

$$G(T) = \frac{2e^2}{h} \sum \frac{\partial f(\epsilon; T)}{\partial \epsilon} \quad (5)$$

$$f(\epsilon) = P_0(T) e^{-\epsilon/t_0} + P_2(T) \frac{1}{\epsilon}$$

$$+ \frac{P_1(T)}{4} [f_s(\epsilon) + 3f_1(\epsilon)] + \frac{1}{m-2} f_m(\epsilon);$$

where $f(\epsilon; T)$ is the Fermi-Dirac distribution, $P_1(T)$ is the thermal probability of finding the local level occupied by 1 electron,

$$P_1(T) = \frac{2}{Z} e^{-\frac{0 - eV_g}{k_B T}}; P_2(T) = \frac{1}{Z} e^{-\frac{2 - 0 - 2eV_g + U}{k_B T}};$$

$$P_0(T) = \frac{1}{Z}; Z = 1 + 2e^{-\frac{0 - eV_g}{k_B T}} + e^{-\frac{2 - 0 - 2eV_g + U}{k_B T}}; \quad (6)$$

In Fig. 3 we plot the conductance as a function of the gate voltage for several values of T . The local level ϵ_0 is below and close to the band bottom, $\epsilon_0 + U$ is above it, and $t^0 \approx t_0$, reflecting the localized nature of the level. The value of $t_0 = \epsilon_0$ corresponds to the number of channels. A 0.75 shoulder is clearly seen at high temperatures $T > T_K$, meanwhile it is complemented to 1 at low temperatures $T < T_K$. This accounts for the basic features observed in the recent experiment [14].

At low temperatures P_1 and $f(\epsilon)$ can be approximated with step functions and for $2\epsilon_0 < eV_g < \epsilon_0 + U$, Eq. (5) becomes

$$G(T) = \frac{2e^2}{h} \left[\frac{3}{4} + \frac{1}{4} F(\tilde{T}) \right]; \quad (7)$$

where $F(\tilde{T})$ is a universal function of rescaled temperature $\tilde{T} = T/T_K$, describing the influence of the Kondo effect. Here, the range of F is $[0; 1]$, the prefactor of F is $1/4$ and the constant is $3/4$, reflecting the fact that the formation of the Kondo singlet involves only the contribution from the singlet channel. In Ref. [14], the same functional form as Eq.(7) is used for $G(T)$, however, the corresponding prefactor and constant are both $1/2$. But the range in which the measured points can be fitted well by a universal function is only from $\tilde{T}=2$ to 1, as can be seen from Fig. 2(b) in Ref. [14]. This implies that the experimental data only confirm the $1/4$ of the conductance that is influenced by the Kondo effect. The other $1/4$ may also vary with temperature but perhaps due to other physical influences. In Ref. [17], from the data of quantum dots the prefactor is 1 and the constant is 0, implying the full Kondo effect for the tunneling. This may indicate the consequence of different structures between a QPC and a quantum dot: the Kondo impurity is an extra local level in QPC as studied in this work while it may be embedded in the tunneling path in quantum dots. It is known that there is no anti-resonance associated with the latter case [19]. It is easy to see that at low T $F(\tilde{T}) \approx 1$ $G(T) = \frac{2e^2}{h} \tanh(\tilde{T} = \frac{T}{T_K})^2$. In the lower inset of Fig. 3 we show (solid line) the scaling conductance of Eq.(7). For a comparison, the experimentally obtained scaling conductance (dashed line) is also shown. The experimental conductance is obtained from

Eq.(1) and Eq.(2) of Ref. [14]. The experimental T_K is twice the value of the theoretical one.

By applying a bias voltage V_b between two leads the current is $I = \frac{2e}{h} \int d\epsilon [f(\epsilon - eV_b/2) - f(\epsilon + eV_b/2)]$, function $F(\tilde{T})$ in Eq.(7) becomes $F(\tilde{T}) \exp[-(eV_b/w)^2]$, reflecting the width $w \approx k_B T_K$ of the Kondo peak in the spectral density [20]. We calculate the differential conductance $g = \frac{dI}{dV_b}$, shown in the upper inset of Fig. 3. The zero-bias peak, originated from the Fermi-level dependence of the Kondo effect, exists only at low temperatures for which the 0.7 shoulder is complemented to 1. By applying a magnetic field, the degeneracy of spins is lifted, and the spin of the local level is along the field direction. As a result, the singlet-triplet representation is no longer suitable and all the plateaus become multiples of $0.5 (2e^2/h)$ due to the splitting of spin subbands.

In summary, we demonstrate that a combination of anti-resonance of the singlet channel and Kondo physics provides a satisfying account of basic features associated with the "0.7 anomaly" in quantum point contacts.

We thank Junren Shi for helpful conversations. This work is supported by DOE Grant No. DE-FG02-04ER46124, NSF-EPSCoR, and NSF-China.

-
- [1] B.J. van Wees et al., Phys. Rev. Lett. 60, 848 (1988).
 - [2] D.A. Wharam et al., J. Phys. C 21, L209 (1988).
 - [3] K.J. Thomas et al., Phys. Rev. Lett. 77, 135 (1996).
 - [4] K.J. Thomas et al., Phys. Rev. B 58, 4846 (1998).
 - [5] A.Kristensen et al., Physica (Amsterdam) 249B -251B, 180 (1998).
 - [6] K.S. Pyshkin et al., Phys. Rev. B 62, 15842 (2000).
 - [7] D.J. Reilly et al., Phys. Rev. B 63, 121 311 (2001).
 - [8] K. Hashimoto et al., Jpn. J. Appl. Phys. 40, 3000 (2001).
 - [9] B. Spivak and F. Zhou, Phys. Rev. B 61, 16730 (2000).
 - [10] V.V. Flambaum and M. Yu. Kuchiev, Phys. Rev. B 61, R7869 (2000).
 - [11] T. Rejcek, A. Ramak and J.H. Jefferson, Phys. Rev. B 62, 12985 (2000); *ibid.* 67, 075311 (2003).
 - [12] C.K. Wang and K.F. Berggren, Phys. Rev. B 57, 4552 (1998).
 - [13] H. Bruus, V.V. Cheianov, and K. Flensberg, Physica (Amsterdam) 10E, 97 (2001).
 - [14] S.M. Cronenwett et al., Phys. Rev. Lett. 88, 226805 (2002).
 - [15] Y. Meir, K. Hirose, and N.S. Wingreen, Phys. Rev. Lett. 89, 196802 (2002); *ibid.* 90, 026804 (2003).
 - [16] Shi-Jie Xiong and Ye Xiong, Phys. Rev. Lett. 83, 1407 (1999).
 - [17] D. Goldhaber-Gordon et al., Phys. Rev. Lett. 81, 5225 (1998).
 - [18] T.A. Costi, Phys. Rev. Lett. 85, 1504 (2000).
 - [19] X.R. Wang, Yupeng Wang, and Z.Z. Sun, Phys. Rev. B 65, 193402 (2002).
 - [20] T.K. Ng and P.A. Lee, Phys. Rev. Lett. 61, 1768 (1988); L.I. Glazman and M.E. Raikh, JETP Lett. 47, 452 (1988); Y. Meir, N.S. Wingreen, P.A. Lee, Phys. Rev. Lett. 70, 2601 (1993).